can be easily generalized on the case of non-uniform deformation for description of the shock wave processes in metals.

Acknowledgement. The work is supported by the Ministry of Education and Science of the Russian Federation, state task 3.2510.2017/PP.

References

1. Kanel, G.I., Zaretsky, E.B., Razorenov, S.V., Ashitkov, S.I., Fortov, V.E.: Unusual plasticity and strength of metals at ultra-short load durations. Phys. Usp. **60**(5), 490–508 (2017)
2. Matsuda, T., Sano, T., Arakawa, K., Sakata, O., Tajiri, H., Hirose, A.: Femtosecond laser-driven shock-induced dislocation structures in iron. Appl. Phys. Express **7**, 122704 (2014)
3. Agranat, M.B., Ashitkov, S.I., Komarov, P.S.: Metal behavior near theoretical ultimate strength in experiments with femtosecond laser pulses. Mech. Solids **49**(6), 643–648 (2014)
4. Smith, R.F., Eggert, J.H., Rudd, R.E., Swift, D.C., Bolme, C.A., Collins, G.W.: High strain-rate plastic flow in Al and Fe. J. Appl. Phys. **110**(12), 123515 (2011)
5. Mayer, A.E., Khishchenko, K.V., Levashov, P.R., Mayer, P.N.: Modeling of plasticity and fracture of metals at shock loading. J. Appl. Phys. **113**(19), 193508 (2013)
6. Borodin, E.N., Mayer, A.E.: Theoretical interpretation of abnormal ultrafine-grained material deformation dynamics. Model. Simul. Mater. Sci. Eng. **24**(2), 025013 (2016)
7. Krasnikov, V.S., Mayer, A.E.: Influence of local stresses on motion of edge dislocation in aluminum. Int. J. Plast. **101**, 170–187 (2018)
8. Bringa, E.M., Rosolankova, K., Rudd, R.E., Remington, B.A., Wark, J.S., Duchaineau, M., Kalantar, D.H., Hawreliak, J., Belak, J.: Shock deformation of face-centred-cubic metals on subnanosecond timescales. Nat. Mater. **5**, 805–809 (2006)
9. Norman, G.E., Yanilkin, A.V.: Homogeneous nucleation of dislocations. Phys. Solid State **53**(8), 1614–1619 (2012)
10. Plimpton, S.: Fast parallel algorithms for short-range molecular dynamics. J. Comput. Phys. **117**, 1–19 (1995). http://lammps.sandia.gov
11. Apostol, F., Mishin, Y.: Interatomic potential for the Al-Cu system. Phys. Rev. B **83**, 054116 (2011)
12. Mendelev, M.I., Underwood, T.L., Ackland, G.J.: Development of an interatomic potential for the simulation of defects, plasticity, and phase transformations in titanium. J. Chem. Phys. **145**(1), 154102 (2016)
13. Sun, D.Y., Mendelev, M.I., Becker, C.A., Kudin, K., Haxhimali, T., Asta, M., Hoyt, J.J., Karma, A., Srolovitz, D.J.: Crystal-melt interfacial free energies in HCP metals: a molecular dynamics study of Mg. Phys. Rev. B **73**, 024116 (2006)
14. Chamati, H., Papanicolaou, N.I., Mishin, Y., Papaconstantopoulos, D.A.: Embedded-atom potential for Fe and its application to self-diffusion on Fe(100). Surf. Sci. **600**, 1793 (2006)
15. Stukowski, A.: Visualization and analysis of atomistic simulation data with OVITO–the Open Visualization Tool. Model. Simul. Mater. Sci. Eng. **18**, 015012 (2010). http://www.ovito.org
16. Stukowski, A., Bulatov, V.V., Arsenlis, A.: Automated identification and indexing of dislocations in crystal interfaces. Model. Simul. Mater. Sci. Eng. **20**, 085007 (2012)
17. Krasnikov, V.S., Mayer, A.E.: Plasticity driven growth of nanovoids and strength of aluminum at high rate tension: Molecular dynamics simulations and continuum modeling. Int. J. Plast. **74**, 75–91 (2015)

Scattering of Waves by a Shear Band

Davide Bigoni[1], Domenico Capuani[2(✉)], and Diana Giarola[1]

[1] DICAM, University of Trento, Via Mesiano 77, 38123 Trento, Italy
[2] DA, University of Ferrara, Via Quartieri 8, 44121 Ferrara, Italy
domenico.capuani@unife.it

Abstract. The incremental behaviour of a prestressed, elastic, anisotropic and incompressible material is analyzed in the dynamic regime, under the plain strain condition. Dynamic perturbations of stress/deformation incident wave fields, caused by a shear band of finite length, formed inside the material at a certain stage of continued deformation, are investigated. At the base of the proposed dynamic perturbation approach is the time-harmonic infinite-body Green's function for incremental displacements obtained by Bigoni and Capuani [5] for small isochoric and plane deformation superimposed upon a nonlinear elastic and homogeneous strain. The integral representation relating the incremental stress at any point of the medium to the incremental displacement jump across the shear band faces, is obtained. Finally, a numerical procedure based on a collocation method is used to solve the boundary integral equation for incident wave scattering by a shear band.

Keywords: Shear band · Wave propagation · Pre-stress · Non-linear elasticity Integral representation

1 Introduction

Localized deformations in the form of shear bands are known to be preferential near-failure deformation modes of ductile materials. The development of shear localization bands has been also shown to be possible in anisotropic composite materials consisting of random distributions of aligned rigid fibres of elliptical cross section in a soft elastomeric matrix [1].

When a ductile material is subject to severe strain, failure is preluded by an emergence of shear bands which initially nucleate in a small area, but quickly extend rectilinearly and accumulate damage, until they degenerate into fractures. Therefore, research on shear bands yields a fundamental understanding of the intimate rules of failure, so that it may be important in the design of new materials.

Modelling a shear band as a slip plane embedded in a highly prestressed material and perturbed by a mode II incremental strain, reveals that a highly inhomogeneous and strongly focussed stress state is created in the proximity of the shear band and aligned parallel to it. This evidence, together with the fact that the incremental energy release rate blows up when the stress state approaches the condition for ellipticity loss, may explain why shear bands grow rectilinearly and why they are a preferred mode of failure [2].

E. E. Gdoutos (Ed.): ICTAEM 2018, SI 5, pp. 279–288, 2019.
https://doi.org/10.1007/978-3-319-91989-8_61

Although it is expected that dynamic effects play an important role on shear band growth, most of the analyses conducted so far were limited to quasi-static conditions. The aim of the present paper is to investigate dynamic perturbations of stress/deformation incident wave fields, caused by a shear band of finite length, formed inside the material at a certain stage of continued deformation. The incremental behaviour of a prestressed, elastic, anisotropic and incompressible material is analyzed in the dynamic regime, under the plain strain condition. The integral representation relating the incremental stress at any point of the medium to the incremental displacement jump across the shear band faces, is obtained, and a numerical procedure, based on a collocation method, is used to solve the boundary integral equation for incident wave scattering by a shear band. The proposed approach provides a basis for the analysis of propagation of disturbances near the boundary of loss of ellipticity. Depending on the level of prestress and anisotropy, wave patterns are shown to emerge, with focussing of signals in the direction of shear bands. Varying the direction of the dynamic perturbation excites different wave patterns, which tend to degenerate to families of plane waves parallel to the shear bands, when the elliptic boundary is approached.

2 Constitutive Equations

The incremental behaviour of an infinite, incompressible, nonlinear elastic material, homogeneously deformed under the plane strain condition, is considered. According to Biot [3], the constitutive relations between the nominal stress increment $\dot{t}_{ij}$ and the gradient of incremental displacement $v_{i,j}$ (a comma denotes partial differentiation) can be expressed in the principal reference system of Cauchy stress (here denoted by axes x_1 and x_2) as follows

$$\dot{t}_{ij} = \mathbb{K}_{ijkl} v_{l,k} + \dot{p}\delta_{ij} \tag{1}$$

where repeated indices are summed and range between 1 and 2, δ_{ij} is the Kronecker delta, $\dot{p}$ is the incremental in-plane hydrostatic stress and $\mathbb{K}_{ijkl}$ are the instantaneous moduli. These moduli possess the major symmetry $\mathbb{K}_{ijkl} = \mathbb{K}_{klij}$ and are functions of the principal components of Cauchy stress, σ_1 and σ_2, describing the pre-stress, and of two incremental moduli μ and μ_* (which can depend arbitrarily on the current stress and strain) corresponding to shearing parallel to, and at 45° to, the principal stress axes. The non-null components are:

$$\begin{gathered}\mathbb{K}_{1111} = \mu_* - \frac{\sigma}{2} - p, \quad \mathbb{K}_{1122} = \mathbb{K}_{2211=} - \mu_*, \quad \mathbb{K}_{2222} = \mu_* + \frac{\sigma}{2} - p \\ \mathbb{K}_{1212} = \mu + \frac{\sigma}{2}, \quad \mathbb{K}_{1221} = \mathbb{K}_{2112} = \mu - p, \quad \mathbb{K}_{2121} = \mu - \frac{\sigma}{2}\end{gathered} \tag{2}$$

with

$$\sigma = \sigma_1 - \sigma_2, \quad p = \frac{\sigma_1 + \sigma_2}{2}. \tag{3}$$

Equation (1) is complemented by the incompressibility constraint for incremental displacement v_i

$$v_{i,i} = 0. \tag{4}$$

Constitutive Eqs. (1)–(4) describe a broad class of material behaviours, including all possible elastic incompressible materials which are isotropic in an initial state, but also materials which are orthotropic with respect to the current principal stress directions. The latter situation has interesting practical applications in the field of fibre-reinforced elastic materials.

3 The Boundary Value Problem

Let S be a shear band of finite length, formed inside the infinite medium at a certain stage of continued deformation. A shear band of finite length can be seen as a very thin layer of material across which the normal component of incremental displacement and of nominal traction remain continuous, but the incremental nominal tangential traction vanishes, while the corresponding displacement is not prescribed. Therefore, it is possible to model such a shear band as a weak surface whose faces can freely slide, but are constrained to remain in contact. Note that this slip surface is different from a crack since it can carry normal tractions, so that only under special symmetry conditions on the prestress state it may behave as a crack subjected to shear parallel to it (the so-called "mode II" loading in fracture mechanics).

In Fig. 1 a shear band of total length $2l$ is represented together with a local reference system $(\widehat{x}_1, \widehat{x}_2)$ centered on the shear band, with $\widehat{x}_1$-axis aligned parallel to the shear band, and rotated at an angle $\theta = \theta_0$ (taken positive when anticlockwise) with respect to the principal reference system (x_1, x_2) introduced for the constitutive Eq. (1).

Introducing the jump operator for a generic function f, smooth on two regions labeled "+" and "−", and discontinuous across the surface S, as

$$[\![f]\!] = f^+ - f^- \tag{5}$$

where $f^{\pm}$ denote the limits approached by function f at the faces of the discontinuity surface, the boundary conditions at the shear band surface S can be written as

$$[\![\widehat{v}_2]\!] = 0, \quad [\![\widehat{t}_{22}]\!] = 0, \quad \widehat{t}_{21} = 0 \tag{6}$$

with $\widehat{v}_i$, $\widehat{t}_{ij}$ being incremental displacement and incremental stress components in the local reference system.

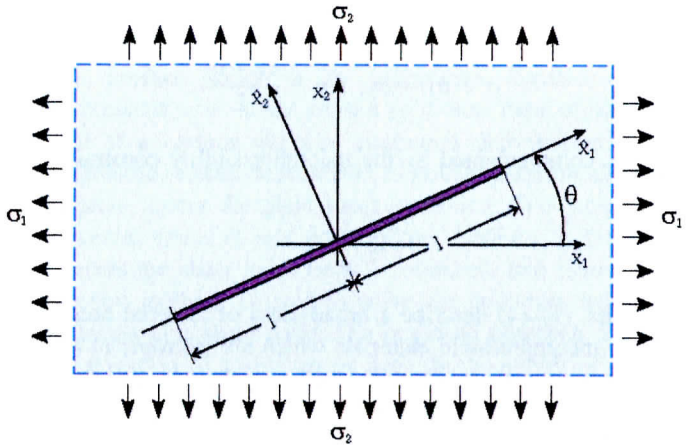

Fig. 1. Shear band of finite length ($2l$) and principal Cauchy stress components, σ_1 and σ_2.

In the hypothesis of time harmonic motion with circular frequency Ω, a wave characterized by an incremental displacement field $v_i^{inc}(\mathbf{x})e^{-i\Omega t}$ travels through the medium and is incident upon the shear band. Then, a scattered incremental displacement field $v_i^{sc}(\mathbf{x})e^{-i\Omega t}$ is generated by the interaction of the incident wave with the shear band such that the total incremental displacement field $v_i(\mathbf{x})e^{-i\Omega t}$ is given by

$$v_i = v_i^{inc} + v_i^{sc} \tag{7}$$

The scattered field v_i^{sc} must satisfy the radiation condition at infinity and conditions of finiteness of energy near the shear band edge. Outside the shear band, the incremental displacement field satisfies the equations of motion

$$\begin{aligned}(2\mu_* - \mu)v_{1,11} + \left(\mu - \frac{\sigma}{2}\right)v_{1,22} &= -\dot{\pi}_{,1} - \rho\Omega^2 v_1 \\ (2\mu_* - \mu)v_{2,22} + \left(\mu + \frac{\sigma}{2}\right)v_{2,11} &= -\dot{\pi}_{,2} - \rho\Omega^2 v_2\end{aligned} \tag{8}$$

where ρ is the mass density and $\dot{\pi}$ is the increment of in-plane nominal hydrostatic stress

$$\dot{\pi} = \frac{\dot{t}_{11} + \dot{t}_{22}}{2} - \frac{\sigma}{2}v_{1,1} \tag{9}$$

Introducing the stream function $\psi(\mathbf{x})$ as

$$v_1 = \psi_{,2}, \quad v_2 = -\psi_{,1} \tag{10}$$

and the dimensionless prestress parameter

$$k = \frac{\sigma}{2\mu}, \tag{11}$$

Equation (8) can be combined to give

$$(1+k)\psi_{,1111} + 2\left(2\frac{\mu_*}{\mu} - 1\right)\psi_{,1122} + (1-k)\psi_{,2222} = -\frac{\varrho\Omega^2}{\mu}\left(\psi_{,11} + \psi_{,22}\right). \tag{12}$$

Equation (12) provides the regime classification, which is the same as for the quasi-static case (see Bigoni and Capuani [4]). The results in this paper will be restricted to the elliptic regime (E), defined through the condition that scalars γ_1 and γ_2

$$\left.\begin{matrix}\gamma_1 \\ \gamma_2\end{matrix}\right\} = \frac{1 - 2\mu_*/\mu \pm \sqrt{\Delta}}{1+k}, \quad \Delta = k^2 - 4\frac{\mu_*}{\mu} + 4\left(\frac{\mu_*}{\mu}\right)^2 \tag{13}$$

are either both real and negative in the elliptic imaginary regime (EI) or a conjugate pair in the elliptic complex regime (EC). Note that Δ is positive in (EI) and negative in (EC).

A consequence of the above discussion is that the emergence of weakly discontinuous surfaces in the medium corresponds to failure of ellipticity, in the present context as in the quasi-static case. This occurs in a continuous loading path (starting from E) either when $k = 1$ (so that $\gamma_1 = 0$) or when $\Delta = 0$ (so that $\gamma_1 = \gamma_2$). The former case defines the elliptic-imaginary/parabolic boundary, while the latter the elliptic-complex/hyperbolic boundary.

4 Integral Representation

With reference to any given point $\mathbf{y}$ outside the shear band, the scattered field can be given the following integral representation in terms of jumps of incremental displacements and incremental stress across the discontinuity surface

$$v_g^{sc}(\mathbf{y}) = -\int_S \left([[\dot{t}_{ij}]] n_i v_j^g(\mathbf{x},\mathbf{y}) - \dot{t}_{ij}^g(\mathbf{x},\mathbf{y}) n_i [[v_j]] \right) dl_x \tag{14}$$

where $\mathbf{n}$ is the unit normal at every point of S, $v_j^g(\mathbf{x},\mathbf{y})$ is the incremental displacement of the time-harmonic Green function for the infinite prestressed medium found by Bigoni and Capuani [5], and $\dot{t}_{ij}^g(\mathbf{x},\mathbf{y})$ is the associated nominal stress increment. In Eq. (14), due to the continuity of the incident incremental field (v_i^{inc}, $\dot{t}_{ij}^{inc}$), jumps of the total incremental field ($[[v_i]]$, $[[\dot{t}_{ij}]]$) coincide with jumps of the scattered incremental field ($[[v_i^{sc}]]$, $\left[\left[\dot{t}_{ij}^{sc}\right]\right]$).

Owing to boundary conditions (6),

$$[[\dot{t}_{ij}]]n_i = 0 \tag{15}$$

so that Eq. (14) reduces to

$$\dot{v}_g^{sc}(\mathbf{y}) = \int_S \dot{t}_{ij}^g(\mathbf{x},\mathbf{y}) n_i [[\dot{v}_j]] dl_x. \tag{16}$$

The gradient of incremental displacement can be evaluated from (16) as

$$\dot{v}_{g,k}^{sc}(\mathbf{y}) = -\int_S \dot{t}_{ij,k}^g(\mathbf{x},\mathbf{y}) n_i [[\dot{v}_j]] dl_x, \tag{17}$$

and the incremental stress can be deduced from constitutive Eq. (1):

$$\dot{t}_{lm}^{sc}(\mathbf{y}) = -\mathbb{K}_{lmkg} \int_S \dot{t}_{ij,k}^g(\mathbf{x},\mathbf{y}) n_i [[\dot{v}_j]] dl_x + \dot{p}\delta_{lm}. \tag{18}$$

In order to determine the incremental displacement jump $[[\dot{v}_i]]$, Eq. (18) is to be written for $\mathbf{y}$ approaching a point of S, where the boundary conditions (6) are prescribed. Denoting by $\mathbf{s}$ the unit tangent vector at any point of S, boundary condition (6_3) can be rewritten as

$$\mathbf{n} \cdot \dot{\mathbf{t}}^{sc}\mathbf{s} = -\mathbf{n} \cdot \dot{\mathbf{t}}^{inc}\mathbf{s} \tag{19}$$

Hence, using the incremental stress representation (18) into boundary condition (19), leads to

$$\mathbf{n} \cdot \dot{\mathbf{t}}^{inc}\mathbf{s} = n_l s_m \mathbb{K}_{lmkg} \int_S \dot{t}_{ij,k}^g(\mathbf{x},\mathbf{y}) n_i [[\dot{v}_j]] dl_x. \tag{20}$$

Equation (20) represents the boundary integral formulation for the boundary value problem at hand. The kernel of the integral Eq. (20) is hypersingular of order r^{-2} as $r \to 0$, r being the distance between field point $\mathbf{x}$ and source point $\mathbf{y}$:

$$r = |\mathbf{x} - \mathbf{y}| = \sqrt{(x_1 - y_1)^2 + (x_2 - y_2)^2} \tag{21}$$

Therefore, the integral on right-hand side of (20) is specified in the finite-part Hadamard sense.

Equation (20) can be given a more explicit expression by introducing the relations for the incremental displacement components in both the principal reference system (x_1, x_2) and the local reference system $(\hat{x}_1, \hat{x}_2)$:

$$\mathbf{v} = \mathbf{Q}\hat{\mathbf{v}}, \quad [\mathbf{Q}] = \begin{bmatrix} \cos\theta_0 & \sin\theta_0 \\ -\sin\theta_0 & \cos\theta_0 \end{bmatrix} \tag{22}$$

so that, due to boundary condition (6_1),

$$[[\dot{v}_j]] = Q_{j1}[[\hat{\dot{v}}_1]] = s_j[[\hat{\dot{v}}_1]]. \tag{23}$$

By using Eqs. (23), (20) can be given the final form

$$\mathbf{n} \cdot \dot{\mathbf{t}}^{inc}\mathbf{s} = n_l s_m \mathbb{K}_{lmkg} \int_S \dot{t}_{ij,k}^g(\mathbf{x},\mathbf{y}) n_i s_j [[\hat{\dot{v}}_1]] dl_x \tag{24}$$

showing that the solution of the problem is given by a linear integral equation in the unknown scalar function $[[\hat{\dot{v}}_1]]$, i.e. the jump of tangential incremental displacement across the shear band faces.

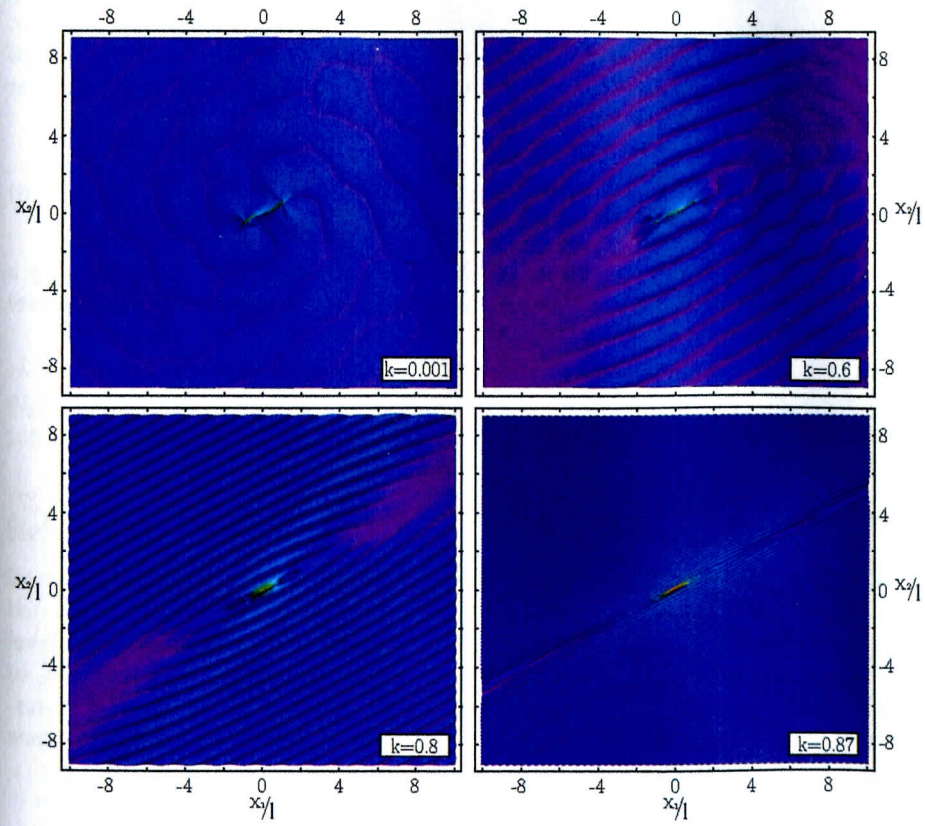

Fig. 2. Real part of scattered incremental deviatoric strain at different prestress levels.

In the particular case $\theta_0 = 0$, Eq. (24) becomes

$$\dot{t}_{21}^{inc} = \int_S \left[(\mu - p)\dot{t}_{21,1}^{2}(\mathbf{x}, \mathbf{y}) + \left(\mu - \frac{\sigma}{2}\right)\dot{t}_{21,2}^{1}(\mathbf{x}, \mathbf{y}) \right] [\![\hat{v}_1]\!] dl_x. \tag{25}$$

5 Numerical Examples

The boundary integral Eq. (24) is solved by a collocation method. The shear band is divided into Q line elements and a linear variation of the incremental displacement jump $[\![\hat{v}_1]\!]$ is assumed within each line element, with the exception of two line elements situated at the shear band tips, where a square root variation of the incremental displacement jump $[\![\hat{v}_1]\!]$ is considered to take into account the singularity at the shear band tip. In particular, the shear band is discretized with $Q = 100$ line elements to obtain the numerical results shown in this section.

A ductile low-hardening metal, modelled within the J_2-deformation theory [6, 7], with the hardening exponent $N = 0.4$, is considered. In the J_2-deformation theory, which is particularly suited to analyze the loading branch of the constitutive response of ductile metals, the prestress parameter k of Eq. (11), and the orthotropy parameter $\xi = \mu_*/\mu$, are given by the relations

$$k = \frac{\lambda^4 - 1}{\lambda^4 + 1}, \quad \xi = \frac{N(\lambda^4 - 1)}{2(\ln \lambda)(\lambda^4 + 1)} \tag{26}$$

where N is the hardening exponent, and λ is the logarithmic stretch representing a prestrain measure. In the case of $N = 0.4$, failure of ellipticity occurs at a prestress level $k = 0.8753$.

A plane incident wave field is considered, with a wavelength $\lambda_1 = 2\pi l$, where λ_1 corresponds to the wavelength of a plane transverse wave propagating parallel to x_1-axis with propagation speed c, i.e.

$$c = \sqrt{\frac{\mu(1+k)}{\rho}}, \quad \lambda_1 = 2\pi \frac{c}{\Omega} \tag{27}$$

The material dynamic response is shown in terms of level sets of incremental deviatoric strain. Level sets of the real part of incremental deviatoric strain are reported in Fig. 2 for the scattered field and in Fig. 3 for the total field. Depending on the level of prestress and anisotropy, wave patterns are shown to emerge, with focussing of signals in the direction of shear bands. Varying the direction of the dynamic perturbation excites different wave patterns, which tend to degenerate to families of plane waves parallel to the shear bands, when the elliptic boundary is approached.

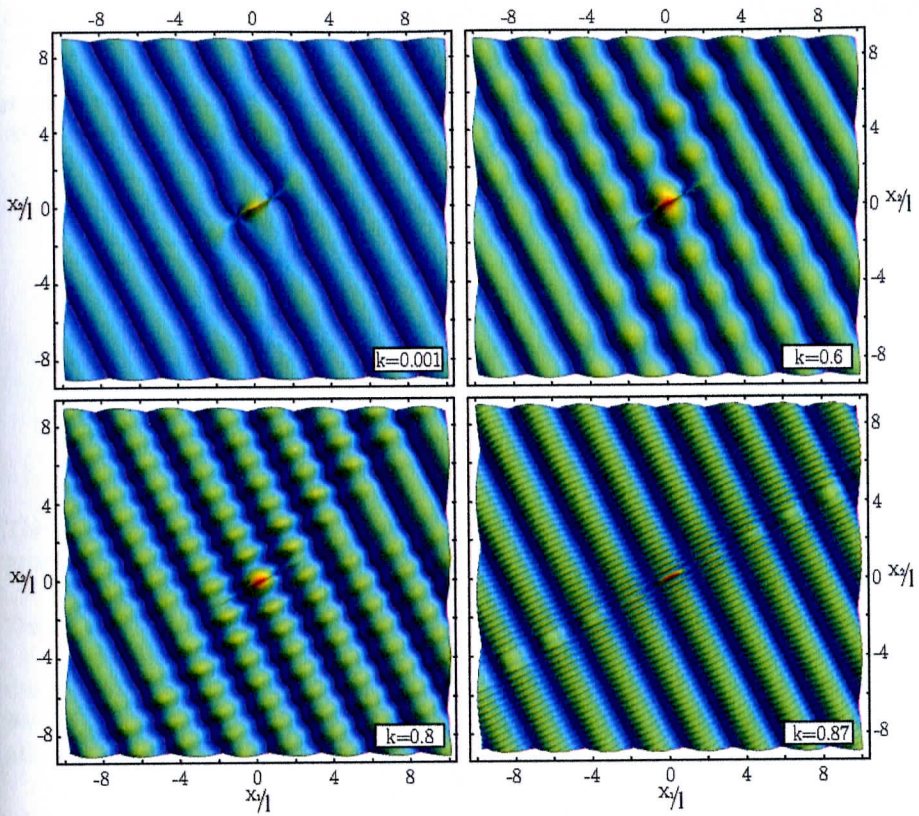

Fig. 3. Real part of total incremental deviatoric strain at different prestress levels.

Acknowledgements. Financial support from the ERC advanced grant ERC-2013-ADG-340561-INSTABILITIES is gratefully acknowledged.

References

1. Avazmohammadi, R., Ponte Castañeda, P.: Macroscopic constitutive relations for elastomers reinforced with short aligned fibers: instabilities and post-bifurcation response. J. Mech. Phys. Solids **97**, 37–67 (2016). https://doi.org/(10.1016/j.jmps.2015.07.007)
2. Bigoni, D., Dal Corso, F.: The unrestrainable growth of a shear band in a prestressed material. Proc. Roy. Soc. A **464**, 2365–2390 (2008). https://doi.org/10.1098/rspa.2008.0029
3. Biot, M.A.: Mechanics of Incremental Deformations. Wiley, New York (1965)
4. Bigoni, D., Capuani, D.: Green's function for incremental nonlinear elasticity: shear bands and boundary integral formulation. J. Mech. Phys. Solids **50**, 471–500 (2002). https://doi.org/10.1016/S0022-5096(01)00090-4
5. Bigoni, D., Capuani, D.: Time-harmonic Green's function and boundary integral formulation for incremental nonlinear elasticity: dynamics of wave patterns and shear bands. J. Mech. Phys. Solids **53**, 1163–1187 (2005). https://doi.org/10.1016/j.jmps.2004.11.007

6. Hutchinson, J.W., Neale, K.W.: Finite strain J_2-deformation theory. In: Carlson, D.E., Shield, R.T. (eds.) Proceedings of the IUTAM Symposium on Finite Elasticity, pp. 237–247. Martinus Nijhoff, The Hague (1979)
7. Argani, L., Bigoni, D., Capuani, D., Movchan, N.V.: Cones of localized shear strain in incompressible elasticity with prestress: Green's function and integral representations. Proc. Roy. Soc. A **470**, 20140423 (2014). https://doi.org/10.1098/rspa.2014.0423

Finite Element Simulation of a Lead-Core Bearing Device Mechanical Response to a Near-Fault Ground Motion

Todor Zhelyazov[1(✉)], Rajesh Ruphakety[2], and Simon Olaffson[2]

[1] Technical University of Sofia, 8 Kliment Ohridski Blvd, 1000, Sofia, Bulgaria
elovar@yahoo.com
[2] Earthquake Engineering Research Center,
University of Iceland, Austurvegur 2a, 800, Selfoss, Iceland
{rajesh, simon}@hi.is

Keywords: Finite element analysis · Strong ground motion
Acceleration time series records · Time-History analysis

The mechanical response of a lead-core bearing device to a real, near-fault, strong ground motion is simulated by performing a finite element analysis.

An explicit 3-D finite element model of the bearing device is built (see Fig. 1). Taking into account some of the existing symmetries, a half-model space is considered.

The following material models are used: linear, elastic and isotropic model (with the assumption that the yield stress will not be reached) – for the steel elements (i); Neo-Hookean model – for the rubber layers (ii); bilinear model with isotropic hardening after yielding - for the lead-core (iii) [1–3].

The strong ground motion is modeled by defining an array that contains the discrete values of the *x*-, *y*- and *z*- components of the support displacements. The elements of the array are obtained on the basis of the recorded acceleration time-series [4, 5] (see Fig. 2).

An approximate solution is obtained by decimating the acceleration time-series. The time domain is divided into substeps of uniform length. The *x*-, *y*- and *z*- components of the acceleration are assumed constant within each substep. The *x*-, *y*- and *z*- components of the velocity and of the acceleration are successively defined by integration of the recorded acceleration time-series. A time-history finite element analysis is then performed.

Three strategies to investigate the mechanical response of the lead-core bearing device seen as a component of a base-isolated structure (i.e. a bridge) are taken into consideration: the bottom side of the bearing device is fixed (e.g. all nodes that belong to the bottom side are constrained) and displacement that model the ground motion are applied to nodes that belong to the top surface as described above (i); point masses are associated to keypoints that belong to one (top or bottom) surfaces of the bearing devices, whereas support displacements are applied to nodes belonging to the other side by using the array defined on the basis of the recorded acceleration time-series (ii); the bearing device is modeled along with a part of the superstructure (iii).